Scale-free avalanches in humans NREM sleep and their relationships with sleep macro and microstructure

Silvia Scarpetta[a,b], Niccolo Morrisi [c], Carlotta Mutti [f], Nicoletta Azzi, Irene Trippi, [f], Rosario Ciliento, Ilenia Apicella[b,d], Marianna Angiolelli[b], Fabrizio Lombardi[e], Liborio Parrino[f], Anna Elisabetta Vaudano[gh]

[a] Department of Physics "E.R.Caianiello", University of Salerno, Italy

[b] INFN, sez. di Napoli, gr. coll. Salerno, University of Salerno, Italy;

[c] Nephrology, Dialysis and transplant unit, university hospital of Modena, Modena, Italy

[d] Department of Physics, University of Naples "Federico II", Italy

[e] Institute of Science and Technology Austria, A-3400 Klosterneuburg, Austria;

[f] Sleep Disorders Center, Department of Medicine and Surgery, University of Parma, Italy;

[g] Neurology Unit, Azienda Ospedaliero-Universitaria of Modena, OCB Hospital, Modena, Italy;

[h]Department of Biomedical, Metabolic and Neural Sciences, University of Modena and Reggio Emilia, Modena, Italy

ABSTRACT

We explore neural avalanches, and the scaling relation among critical exponents, in overnight EEG recordings in human healthy subjects, during NREM sleep. Notably, the distributions of the avalanches' size and duration are well described by a power law, with critical exponents in agreement with mean-field directed percolation class. Moreover, we study the correlation between the avalanches' spatiotemporal structure and the sleep macro and microstructure as reflected by the CAP framework. Overall, our findings provide evidence of a link between the avalanche's occurrence, slow-wave sleep dynamics, sleep stages transitions and CAP-phase A.

INTRODUCTION

Sleep is an active and dynamic complex process regulated by mechanisms which guide the alternating process of non-REM (NREM) and REM stages across the night. Physiologically, sleep macrostructure is characterized by the concentration of deep slow wave sleep (stage N3) in the first part of the night and the dominance of REM sleep and light sleep (mainly N2) in the second half, a balanced skewness modulated by the homeostatic process and by the REM-off and REM-on systems. The cyclic alternating pattern (CAP) is one of the major adaptive components of NREM sleep. According to Terzano and Parrino (2000), CAP is a periodic EEG activity of NREM sleep characterized by repeated spontaneous phases of EEG activation (A phase) and subsequent phases of return to background activity (B phase), evolving in a cycling pattern. Based on the distribution of slow and fast EEG frequencies, the A phases of CAP are classified in three subtypes: A1, A2 and A3 (Terzano et al., 2001). These CAP subtypes are not randomly distributed along the night, but instead their appearance is linked with the homeostatic, ultradian and circadian mechanisms of sleep (Parrino et al. 1993; Terzano et al. 2005). In particular, subtypes A1 are the expression of slow wave sleep propensity and follow the exponential decline of the homeostatic process. A covariance between A1 subtypes and sleep slow wave activity (SWA) has been proposed and the two electroencephalographic elements likely share the beneficial effect on sleep-related cognitive processes (Ferri et al., 2008; Arico et al., 2010). Furthermore, both CAP-A1 subtypes and SWA are involved in the build-up and

maintenance of deep NREM sleep acting as protectors for sleep continuity (Terzano et al. 2000; Parrino and Vaudano, 2018).

Spontaneous alternation of transient synchronized active and quiescent periods is typical of systems that self-organize near a critical point of a non-equilibrium phase transition (Scarpetta and de Candia 2014, Munoz, 2018). At criticality, systems have a number of peculiar properties that could be advantageous to brain functions, such as long-range correlations, maximum variability of spatio-temporal patterns, and wide range of responses to external perturbations [Beggs and Plenz 2003, Petermann et al. 2009, Shew et al. 2015, Ma et al 2019, Chialvo 2010, Shew and Plenz 2013, Massobrio et al Front. Syst. Neurosci 2015]. Such properties would translate into the ability of the brain to efficiently integrate activity across spatial and temporal scales, and promptly and flexibly respond to external stimuli by generating a rich variety of coordinated collective behaviors. Following these arguments and a number of theoretical and numerical results [Shew W., Plenz D. (2013).; Kinouchi O., Copelli M. (2006). Shew W., et al. (2009), Hesse and Gross 2014; Beggs and Timmie, 2012] it has been hypothesized that the brain self-organizes to criticality to maximize information processing and computational capabilities, achieving optimal functional performance. This hypothesis is supported by empirical observations of neuronal avalanches — cascades of neural activity exhibiting power-law size and duration distributions — and long-range spatio-temporal correlations in neural activity across species, systems, and spatial scales (Beggs and Plenz, 2003; Petermann et al., 2009; Tagliazucchi et al, 2012; Palva et al., 2013; Zhengyu et al, 2019; Ribeiro et al, 2021; Lombardi et al., 2020). In particular, presence of power law distributions indicates absence of characteristic temporal and spatial scales in the underlying dynamics, a typical feature of physical systems near the critical point of a phase transition.

In humans, sleep plays a crucial role to re-tune the system towards criticality (Meisel 2013, Meisel 2017). There is evidence (Priesmann et al 2013, Bocaccio 2019, Allegrini et al. 2013, Allegrini et al 2015) that the brain operates close to criticality from wakefulness to deep NREM sleep, with small changes across vigilance states. The normalized mean avalanche size and duration are largest during

slow wave sleep and smallest in REM (Priesmann et al., 2013). These findings, however, disregard the dynamic changes that accompany sleep stage transitions and neglect the complex sleep micro-architecture, composed of arousals (brief wake bouts) and bursts of cortical brain wave activity, occurring at time scales much shorter than the conventional and apparently monolithic sleep stages. Preliminary observations in animal models have pointed out that dual bursts of θ (active phases) and δ (quiescent phases) activity, as expression of sleep microstructure, exhibit typical features of non-equilibrium systems self-organizing at criticality (Wang et al., 2019, F. Lombardi et al 2020).

Herein, we aim to characterize the critical behavior, estimate the critical exponents, and establish the basic mechanisms that underlie cortical dynamics of sleep architecture and sleep microstructure as reflected by the CAP framework.

2. MATERIALS AND METHODS

2.1 PARTICIPANTS

The data analyzed in this study were extracted from overnight polysomnography (PSG) recordings acquired from the Parma (Italy) Sleep Disorders Center database. Ten healthy subjects, 5 males and 5 females, mean aged 39,6 years (age range 28-53), were selected after the accomplishment of an entrance investigation. Subjects were selected based on the following inclusion criteria: (i) absence of any psychiatric, medical and neurological disorder (ii) normal sleep/wake habits without any difficulties in falling or remaining asleep at night: a personal interview integrated by a structured questionnaire confirmed good daytime vigilance level; (iii) no drug intake at the time of PSG and the month before; (iv) full night unattended PSG recordings performed with EOG (2 channels), EEG [Ag/AgCl electrodes placed according to the 10 - 20 International System referred to linked-ear lobes. Recording electrodes were 19 (Fp2, F4, C4, P4, O2, F8, T4, T6, Fz, Cz, Pz, Fp1, F3, C3, P3, O1, F7, T3, T5) in seven subjects and 25 in the remaining three: (CP3, CP4, C5, C6, C2, C1, FC4, FC3, F4, C4, P4, O2, F8, T4, T6, Fz, Cz, Pz, F3, C3, P3, O1, F7, T3, T5), EMG of the submentalis muscle, ECG, and signal for SpO2 (pulse-oximetry O2-saturation).

PSG recordings were acquired using a Brain Quick Micromed System 98 (Micromed, SPA). A calibration of 50 uV was used for EEG channels with a time constant of 0.1 s and a low-pass filter with 30 Hz cut-off frequency. EEG sampling rate was 256 Hz for six subjects while for the remaining four cases, one was recorded using a sampling rate of 128 Hz (case #1) and the remaining three (cases #2, #3, #4) using 512 Hz. Each signal was recorded and examined by an expert clinician (CM, IT, LP). Analysis of sleep recordings (see below) was performed with Embla RemLogic Software. The institutional Ethical Committee Area Vasta Emilia Nord approved the study (protocol nr. 19750).

2.2 SLEEP ANALYSES

2.2.2 Analysis of Sleep Macrostructure

Sleep was scored visually in 30-s epochs using standard rules according to the American Academy of Sleep Medicine (AASM) criteria (Berry RB, Brooks R, Gamaldo C, Harding SM, Llyod RM, Quan SF, et al. AASM scoring manual updates for 2017 (Version 2.4). *J Clin Sleep Med.* (2017) 13:665–6. doi: 10.5664/jcsm.6576). Conventional PSG parameters included total time in bed (TIB) (minutes), total sleep time (TST) (minutes), sleep latency (minutes), rapid eye movement (REM) latency (minutes), sleep efficiency (%), wake after sleep onset (WASO) (minutes), as well as percentage of NREM (N1, N2, N3) and REM stages.

2.2.3 Analysis of Sleep Microstructure

Sleep microstructure evaluation refers to the quantification of CAP parameters based on the published international atlas (Terzano et al., 2001) and was manually performed using Embla REM-logic software by somnologists with strong expertise in the field (LP, CM). CAP is a global EEG phenomenon involving extensive cortical areas, therefore CAP phases should be visible on all or most EEG leads. CAP is characterized by the alternation of phase A (transient electrocortical events) and phase B (low voltage background), both lasting between 2 and 60 seconds. According to published criteria (Terzano et al., 2001) phase A activities were classified into three subtypes:

- **Subtype A1**: EEG synchrony is the predominant activity and the EEG desynchrony occupies < 20% of the whole phase A. Subtype A1 may include delta burst, K-complex sequences, vertex sharp transients, polyphasic bursts with < 20% of EEG desynchrony.
- **Subtype A2**: it is a mixture of fast and slow rhythms where the EEG desynchrony occupies 20-50% of the entire phase A. This subtype includes polyphasic bursts with 20-50% of EEG desynchrony.
- **Subtype A3**: EEG desynchrony is the predominant activity (> 50%) of the phase A. Subtype A3 includes K-alpha, EEG arousal and polyphasic bursts with >50% of EEG desynchrony.

The percentage of NREM sleep occupied by CAP sequences defines the CAP rate. The absence of CAP for >60 seconds is scored as non-CAP, which represents the portion of NREM sleep characterized by a sustained physiologic stability. CAP sequences usually precede sleep stage transitions, and, specifically, subtypes A2 and A3 typically assist the shift from NREM to REM sleep. Under physiologic circumstances, CAP is not present during REM sleep. The following CAP variables were measured:

(i) total CAP time in minutes (total CAP time in NREM sleep),

(ii) CAP rate (the percentage ratio of CAP time over total NREM sleep),

(iii) number and duration of CAP cycles,

(iv) number and duration of each phase A subtypes (A1, A2, A3),

(v) total number of phase A (derived by the sum of A1+A2+A3),

(vi) duration of phase A and B in seconds.

2.3 DEFINITION FOR AVALANCHES

Before avalanche analysis, waking and motion artifact segments during nocturnal sleep were manually identified and removed.

To capture the spatiotemporal organization in avalanches of transient EEG events during sleep, we investigated clusters of large deflections of the artifact-free EEG signals. For each EEG channel, large positive or negative excursions beyond a threshold were identified, after z-transformation of the signal by subtraction of the mean and dividing by the standard deviation (SD). The aim to detect intervals of large deviations activity is similar to the original works on neuronal avalanches derived from Local Field Potential (LFP) (Beggs and Plenz, 2003; Petermann et al., 2009; Thiagarajan et al., 2010) and from Multiunit Activity (MUA) spike counts (S.H. Gautam et al. (2015)). While for MUA, avalanches were defined as periods of time when the MUA spike count exceeded a positive threshold, and for LFP the excursions were defined for negative potentials due to their close correlation to neuronal spiking, herein, for scalp EEG traces, we considered both positive and negative potentials to identify avalanches in line with previous works on EEG/MEG data (C. Meisel Journal of Neuroscience et al. 2013, E.D. Fagerholm j neuroscet al.. 2015 ,O. Shriki et al Jour Neurosci. 2013). A Gaussian distribution of amplitudes is expected to arise from a superposition of many uncorrelated sources. Conversely, avalanche analyses are expected to generate amplitude distributions that deviate from a Gaussian shape. The comparison of the signal distribution to the best Gaussian fit indicates that the two distributions start to deviate from one another around $\vartheta = \pm 2$ SD (**Fig. 1**). Accordingly, we choose a threshold of $\vartheta = \pm 2$ SD throughout the paper for avalanches' detection (with the exception of Supplementary Material S3 where effects of threshold different from $\vartheta = \pm 2$ SD on avalanche distributions are taken into account).

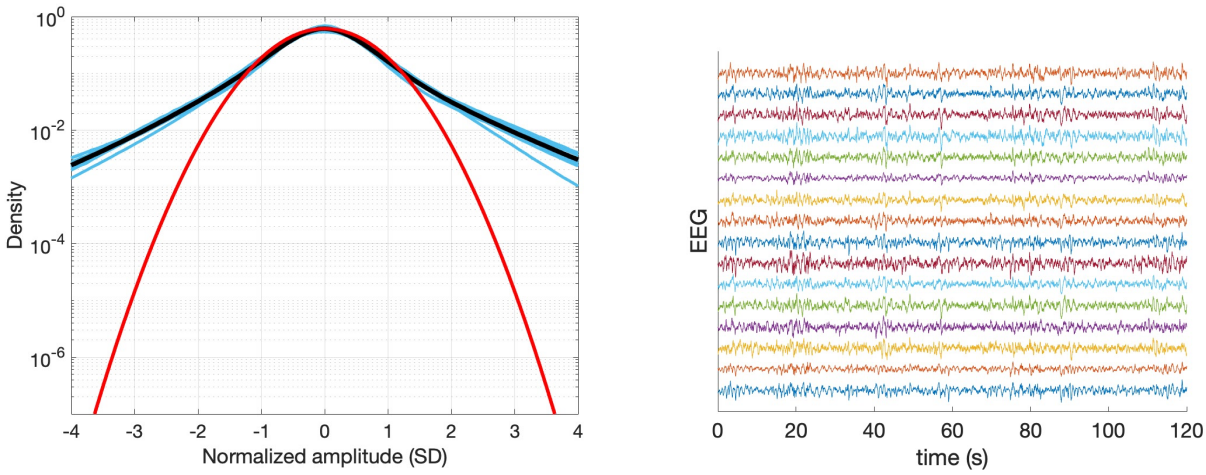

Fig. 1 A) Histogram of the z-transformed EEG signals. The cyan curves in the background are the signal amplitude distributions of all individual 10 subjects (based on all channels). Note that the signal from each sensor was z-normalized by subtracting its mean and dividing by the SD. The black curve is the grand average over all subjects. The red curve is the best fit Gaussian distribution for the grand average. The normalized data histograms start deviating from the Gaussian fit around ±2 SD.
B) A sample of z-transformed EEG for all the channels of subject #1. Signals are vertically translated for clarity.

A cascade is thus defined as a concatenation of fluctuations, namely a continuous interval in which there is at least one supra-threshold channel. We therefore sum over all the channels the supra-threshold fluctuations, and avalanches are defined as periods of time where this sum is consecutively different from zero. Avalanches in this manner are preceded and followed by an "empty" interval (with sum zero) as usually defined in original avalanches' works (Plenz Beggs 2003). Size of the avalanche is then defined as the integral of the sum of the threshold signals.

2.4 STATISTICAL ANALYSIS

We calculated the distribution of avalanches' sizes and durations, and the correlation of the spatiotemporal structure of avalanches with the sleep macrostructure and microstructure measures. Using the "powerlaw" python package (J. Alstott, et al. 2014) we evaluated the statistical significance of a power law fit of the observed avalanches' size and duration distribution and we estimated the exponents. The Kolmogorov-Smirnov distance, *D*, between the data and the fit has been evaluated. We also compute the log-likelihood ratio R of the power-law distribution with respect to an exponential distribution, which leads to a p value that quantifies the significance.

To characterize the relationship between the avalanche dynamics and the sleep macrostructure, we calculate for each subject the avalanche density as a function of time, i.e. the fraction of time occupied by avalanches, measured as

$$F_{av}(t) = \frac{u_{av}(t)}{u_0} \quad (1)$$

where $u_{av}(t)$ is the amount of time occupied by avalanches, in a sliding window of length T, and u_0 = T. The window length T has been chosen equal to 10 seconds (T=10 s) as this is the cut-off in the avalanches' duration distribution, i.e. the order of magnitude of the largest avalanches in our recordings.

To characterize the relationship between the avalanche dynamics and the sleep microstructure, we compute the Pearson correlation coefficient between the avalanches occurrence and the CAP measures, on a time scale dictated by the sampling rate of the recordings.

Given the binary values $x_i = 0,1$, $y_i = 0,1$, where $x_i = 1$ indicates the presence in the sample *i* of an ongoing avalanche, and y_i=1 indicates presence of a particular feature of the CAP framework (CAP, NCAP, subtypes A1, A2, A3, all/global phases A, phases B), we computes the Pearson correlation coefficient as:

$$\rho_{x,y} = \frac{\sum_{i=1}^{N} (x_i - \bar{x})(y_i - \bar{y})}{\sqrt{\sum_{i=1}^{N} (x_i - \bar{x})^2}\sqrt{\sum_{i=1}^{N} (y_i - \bar{y})^2}} \quad (2)$$

where $\bar{x} = \sum_{i=1}^{N} x_i$ and N is the number of samples in the sleep registration.

Being binary values, the Pearson correlation coefficient is equivalent to the phi coefficient.

The Pearson correlation coefficient has been also evaluated between avalanches occurrence and macrostructure stages, using (2) where $x_i = 1$ indicates the presence ($x_i = 0$ absence) in the sample i of an ongoing avalanche, and y_i=1 indicates presence ($y_i = 0$ absence) of a particular sleep stage (REM,N1,N2,N3).

3. RESULTS

Herein, we aim to characterize the critical behavior and establish the basic mechanisms that underlie cortical dynamics of hypnograms architecture and of human sleep microstructure, as reflected by the CAP framework. First, by analyzing overnight polysomnography recordings (PSG), we measured critical signatures such as scale-free avalanches of activity, finding exponents in qualitative agreement with the branching process universality class. Then we focus on the relationship between the dynamics of avalanches' density and the main macrostructure (sleep hypnogram architecture and sleep stages) and on the Pearson correlation coefficient between avalanche occurrence and microstructure (CAP) features of sleep.

The main sleep parameters are described in **Table 1** (macrostructural measures) and **Table 2** (CAP analysis). The average TST across the 10 subjects was 423,9 minutes, with a mean SE of 88,92%. Around 56% of TST was spent in light sleep ($N1 = 7{,}23\%, N2 = 48{,}47\%$,), 30% in deep sleep ($N3 = 30{,}04\%$), and 20,30% in REM. The mean CAP rate was 49,29% with the following distribution across NREM stages: $N1 = 41{,}69\%, N2 = 48{,}36\%$ and $N3 = 55{,}76\%$.

On average, subjects presented 37,1 CAP sequences per night. with a mean duration of 4 minutes and 55 seconds. With respect to CAP subtypes distribution, 225,8 were A1; 207,1 were A2 and 99,35 were A3. Confirming previous studies (Halasz et al., 2014), A1 subtypes were mainly observed

during stage N3 (50,21%) compared to N2 (18,01%) and N1 (1,75%). By contrast, subtypes A2 and A3 predominated in stage N2 (18,01% for A2 and 13,98% for A3).

	MEAN	SD
sleep latency (minutes)	9,90	12,92
SE (%)	88,92	8,80
TST (min)	423,90	69,31
WASO (minutes)	40,97	30,46
Stage N1 (minutes)	28,75	17,47
Stage N1 (%)	7,23	4,95
Stage N2 (minutes)	207,10	50,85
Stage N2 (%)	48,47	6,33
Stage N3 (minutes)	99,35	13,40
Stage N3 (%)	30,40	20,88
NREM sleep (minutes)	335,20	41,67
REM sleep (minutes)	78,65	38,96
REM sleep (%)	20,30	4,88

Table 1: Main macrostructural measures across the 10 subjects (Mean and Standard Deviation (SD)). SE= sleep efficiency(SE), TST= total sleep time, WASO=Wake After Sleep Onset

	MEAN	SD
CAP time (minutes)	162,51	42,3
CAP rate (%)	49,05%	0,1
CAP sequences (n)	37,1	8,3
CAP sequences length (minutes)	4,55	1,6
CAP cycle (n)	357,6	104,1
Phase A length (s)	8,59	1,4
Phase B length (s)	20,67	3,5
Subtype A1 duration (s)	6,42	2,0
Mean time subtype A1 (%)	25,7	11,1
Subtype A2 duration (s)	8,63	2,0
Mean time subtype A2 (%)	9,29	5,8
Subtype A3 duration (s)	12,72	1,32
Mean time subtype A3 (%)	5,76	1,9

Table 2: Main macrostructural measures across the 10 subjects (Mean and Standard Deviation (SD)).

3.1 CRITICAL AVALANCHES DISTRIBUTION AND SCALING RELATION DURING SLEEP

To check if the spatio-temporal structure of avalanche dynamics has a scale-free behavior, we compute the distribution of avalanches' sizes and durations. **Fig.2** shows the distribution for subject #1, while **Fig.3** distribution for all the avalanches of all the subjects.

Notably we found that the distributions are well described by a power law

$P(S) \propto S^{-\tau}$ (3)

$P(T) \propto T^{-\beta}$ (4)

followed by a cut-off, both at single subject and at group-level, indicating that there is scale-invariance , ie. there is not any preferential scale (up to a maximum scale that sets the cut-off). This is a common signature of critical behavior. The black line in **Figs. 2,3** is the power law fit (the length of black line also indicates the range where fitting exponent was estimated) with the maximum likelihood estimator (MLE) as made available in the `powerlaw` python package [J. Alstott, E. et al. (2014)].

The exponents of the power laws fit of single subject's avalanche distribution, in **Fig. 2**, are $\tau = 1.45 \pm 0.01$ for the size and $\beta = 1.89 \pm 0.01$ for the duration similarly, in **Fig. 3**, for all the subjects, exponents of power law fit are $\tau = 1.42 \pm 0.01$ for the size, and $\beta = 1.83 \pm 0.01$ for the duration. We compute the log-likelihood ratio R of the power-law fit with respect to an exponential distribution (always in the range indicated by black line) and we get $R = 333$ for the size and $R = 118$ for the duration distribution in **Fig. 3** (while $R = 62$ for the size and $R = 39$ for the duration distribution of a single subject in **Fig.2**), with *p-value zero* (within machine precision) for both size and duration.

Fig 4. shows (with red stars) the average size of the avalanche $\langle S \rangle(T)$ as a function of its duration T (for the single subject in A, and all the subjects in B). Green dots is the scatter plot of the data $S(T)$. The average size is well described by a power law

$$\langle S \rangle(T) \propto T^k \qquad (5)$$

up to the maximum duration where the cut-off of $P(T)$ starts. The estimated exponent is $k = 2$ (black line in **Fig. 4** A and B), up to large values of *T*. A power law with a lower slope (dotted line with $k = 1.3$ in **Fig. 4**) describes $\langle S \rangle(T)$ only in the region where $P(S)$ and $P(T)$ have the cut-off (compare **Fig. 4** with **Figs. 2,3**), due to finite-size effects. This behavior is observed also in the 10 single subject avalanches distribution, as shown in supplementary material (**Fig. S1**).

Notably the exponent $k = 2$ observed in **Fig.4** is in agreement, within errors, with the value predicted by the scaling relation

$$k = \frac{\beta - 1}{\tau - 1} \qquad (6)$$

This scaling relation, discussed in ref. [J. P. Sethna et al (2001)] in relation to crackling noise, has a general validity in avalanche dynamics, as shown in [Scarpetta et al. 2018, Fosque 2021] where the (6) was derived by a simple reasoning with the only hypothesis that (3) and (4) holds and fluctuations in the size fixed the duration are small and can be neglected. Indeed it has also been derived in relation to the BTW Self-Organized Criticality model in [Jensen Self-Organized Criticality].

Notably, the relation $S(T) \propto T^k$, with (6) satisfied, holds also both experimentally [Friedman et al. 2012, Fontenele et al. 2019, Shew et al. 2015, Mariani et al. 2021] and in some spiking models [Scarpetta et al 2018].

A debated question is if the values of exponents and slope of (5) when scaling relation (6) is experimentally satisfied are compatible with MF-DP values [Miller et al 2019, Fontenele 2019, Carvalho 2021, Fosque 2021]. Herein, the estimated values of the critical exponents τ, β and k are similar to the ones predicted by the branching process theory, i.e. the mean field directed percolation (MF-DP) class, with exponent 1.5 for the size, 2 for the duration distribution and $k = 2$ for $\langle S \rangle(T)$.

To check the robustness of the k=2 exponent in our $\langle S \rangle(T)$ experimental data, we evaluate the behavior of $\langle S \rangle(T)$ when a different threshold is used to define avalanches. The comparison of the signal distribution to the best Gaussian fit in Fig. 1, led us to define avalanche using a threshold of $\vartheta = \pm 2$ SD throughout the paper. In supplementary **Fig. S2** we show distribution P(S) P(T) of size and duration of avalanches, together with shape of $\langle S \rangle(T)$, using a threshold $\vartheta = \pm 1$ SD and $\vartheta = \pm 3$ SD for the avalanche definition. Notably the exponents τ,β, and k in (3,4,5) are all very robust.

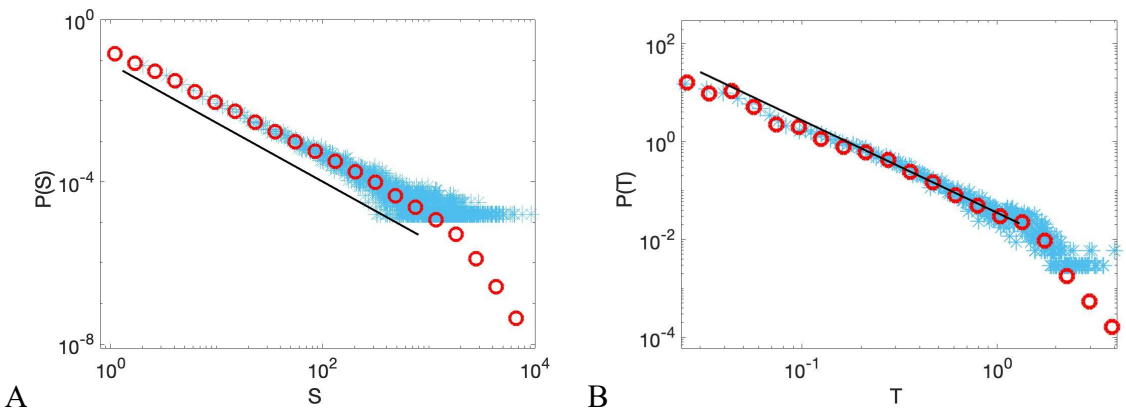

Fig. 2 Distribution of avalanches size (A) and duration (B) in subject #1 (shown with logarithmic binning by red circle and linear binning by light blue crosses). A power law regime is followed by a cut off. The powerlaw python package [J. Alstott, et al. (2014)] was used. The black line indicates the range of data used for the fit, and the slope of the power law fit. For avalanche's size, the fit gives an exponent τ= 1.45 ± 0.01 with a *Kolmogorov-Smirnov distance, D*, between the data and the fit, $D = 0.1$. For the duration the fit gives an exponent β =1.89±0.01 with a Kolmogorov-Smirnov distance between the data and the fit $D = 0.09$. The log-likelihood ratio R of the power-law fit with respect to an exponential distribution (always in the range indicated by black line) is $R = 62$ for the size and $R = 39$ for the duration distribution.

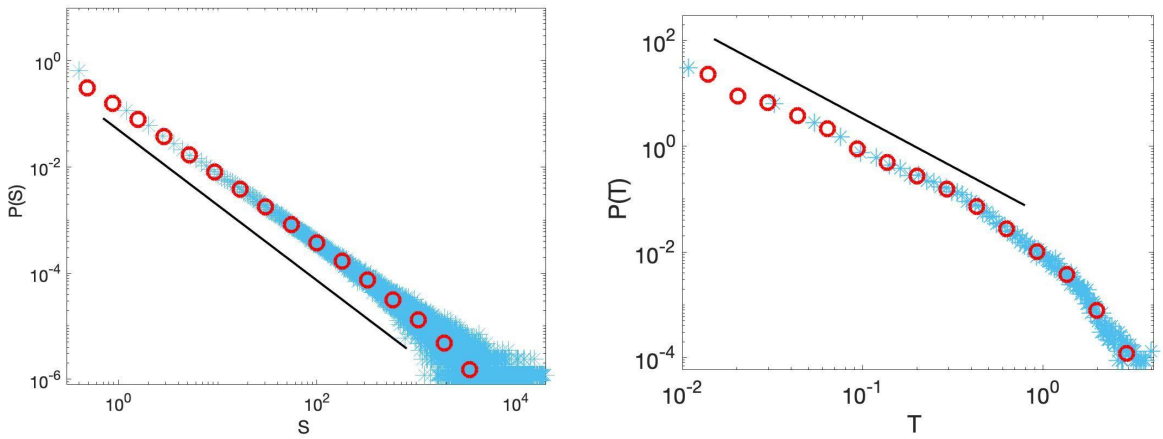

Fig. 3 Distribution of avalanches size (A) and duration (B) over all the subjects (shown with logarithmic binning by red circle and linear binning by light blue crosses). We can observe that a power law regime is followed by a cut off. To estimate the exponents of the power law regime, the `powerlaw` python package [J. Alstott, et al. (2014)] was used. The black line indicates the range of data used for the fit and the slope obtained using the estimated exponent. For avalanche's size, the estimated exponent is τ= `1.42±0.01 with a` Kolmogorov-Smirnov distance, D, between the data and the fit, $D = 0.09$. For the duration the fit gives an exponent β=`1.83±0.01` with a Kolmogorov-Smirnov distance between the data and the fit $D = 0.12$.

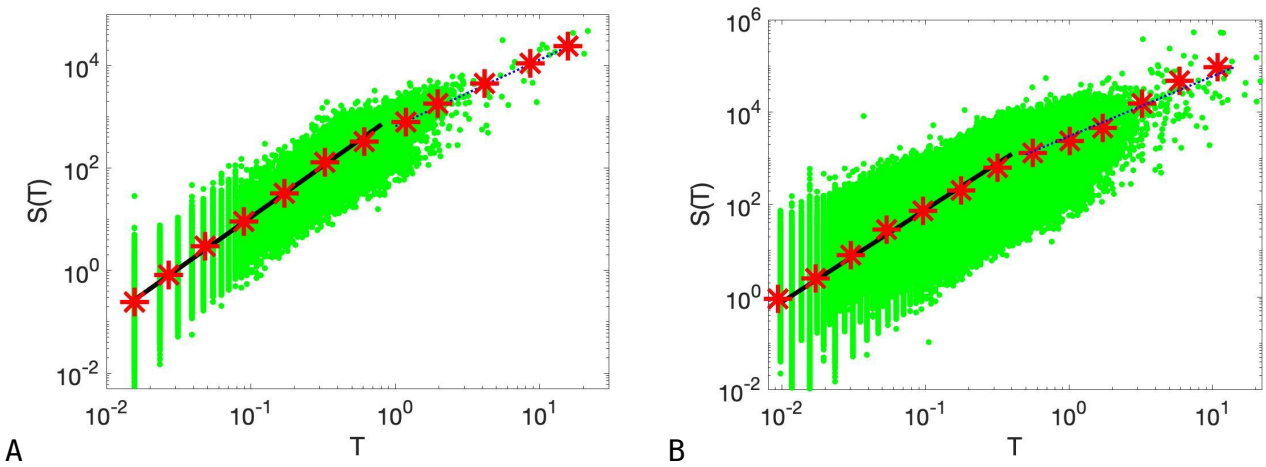

Fig.4 Distribution of avalanches average size $\langle S \rangle(T)$(red stars) as a function of duration T for subject #1(A) and for all subjects (B). Green dots show the (S,T) dataset, and red stars show the average size $\langle S \rangle(T)$ with logarithmic binning in T. A power l aw regime $\langle S \rangle(T) \propto T^k$ with k =2 fit the data up to a maximum duration where the cut off of $P(T)$starts, this regime is followed by a regime with a smaller slope. Black line has a slope k =2, while in the cut-off region the dotted blue line has a slope 1,3 as a guide for eye.

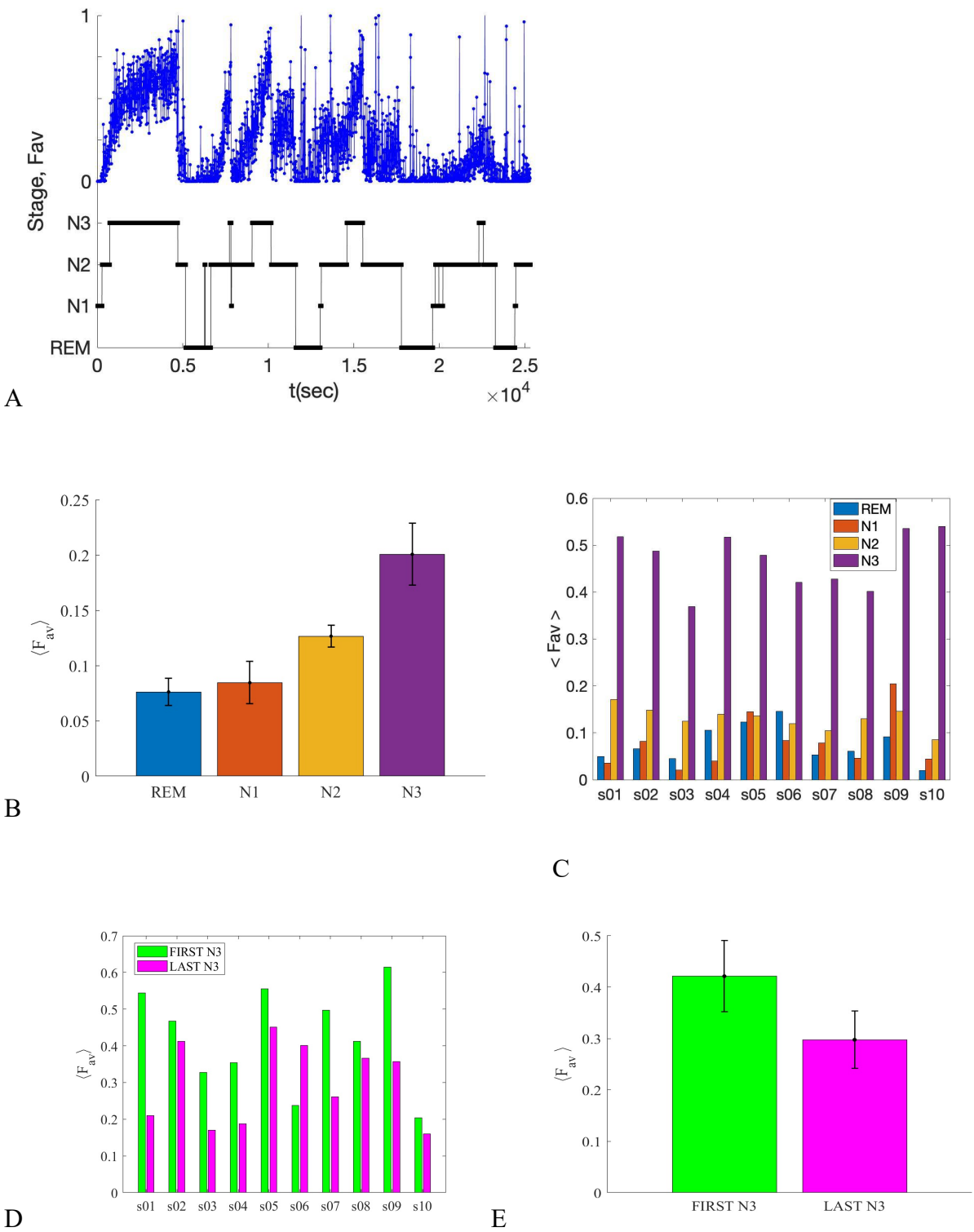

Fig. 5: (**A**) Avalanche's density $F_{av}(t)$ (blue dots) is shown as a function of time, together with the sleep stages (REM, N1, N2, N3 black line), in subject#1. Notably $F_{av}(t)$ increases gradually in N2 and N3, and then abruptly decreases switching from N3 to N2, N1 or REM. Waking periods during sleep have been removed before avalanches' analyses. The mean avalanche density for each sleep stage (REM,N1,N2,N3) is shown, both averaged at group level (Panel **B**), and for each of the 10 subjects (Panel **C**). N3 is the stage with higher density of avalanches. (**D**) Mean density of avalanches in the FIRST N3 and LAST N3 stage of the recording, averaged over all 10 subjects. Bar is the

standard error. (**E**) Average of avalanches' density in the FIRST N3 (green) and LAST N3 (magenta) of the recording, for the 10 subjects. Notice that s 06 presents an opposite behavior, with an increase of avalanches during the LAST N3 sleep cycles. Notably s06 sleep macrostructure was slightly deviant from healthy sleep sleepers, as he presented an unusually short duration of N3 stage at the beginning of the night, followed by a gradual increase of N3 in the second half of his sleep recording, which may justify the atypical behavior of his sleep avalanches.

3.2 AVALANCHES DISTRIBUTION AND SLEEP MACROSTRUCTURE

Fig. 5 describes the distribution of avalanches in relation with the sleep hypnogram and sleep stages. We measure the avalanches' density over time $F_{av}(t)$ defined in (1). $F_{av}(t)$increases gradually in parallel with sleep deepening: it starts very small during stage N1, reaches an intermediate value during stage N2 and increases substantially during stage N3 (see **Fig. 5A** where $F_{av}(t)$ is shown for a representative subject #1). By contrast, the avalanche density decreases quite abruptly when the system switches from N3 to N2 or to N1. Changing perspective, we also noticed that avalanche density gradually increases during the ascending slope of each sleep cycle, whilst it rapidly decreases in the descending slope of the same cycles preceding the onset of REM sleep.

Fig. 5.B,C shows the density of avalanches $\langle F_{av} \rangle$ averaged over the different sleep stages, both at single subject and group level. The avalanche density reaches the highest values in N3.

Indeed (see **Fig. 5A**) we also observed a strong linear positive correlation between the time spent in N3 and the avalanches's density $F_{av}(t)$. This relationship suggests that the mechanisms related with the density of avalanches become more and more effective during SWS and moves the systems towards the deepest stages of sleep.

Avalanche's density peak was usually higher in the first half of the night and progressively decreased in the last part of recording.. We then compare statistics of avalanches in the first N3 stage with those in the last N3 of the overnight sleep. While avalanches' size and duration distributions in first N3 are qualitatively comparable to that of last N3 (see supplementary information **Fig. S3**), we observe a difference in avalanche density. In **Fig. 5D,E** the density of avalanches $\langle F_{av} \rangle$averaged over the first N3 is compared with the density $\langle F_{av} \rangle$on the last N3, for all 10 subjects. In all subjects, except subject #6, the first N3 stage has a larger avalanche density than the last N3 stage. An unpaired two-sample

t-test rejects the hypothesis that the two densities (in the first and last N3) come from distributions with equal means (with unknown and unequal variances), with a p-value $p = 0.04$.

Finally we evaluate the Pearson correlation coefficient between the avalanche occurrence and the presence of a particular sleep stage, using eq. (2) with y_i=1 indicating the presence (y_i=0 absence) of a particular sleep stage (REM,N1,N2,N3), and x_i=1 the presence (x_i=0 absence) of an avalanche in the i-th sample. Results shown in Fig. 6 shows a very small (negative) correlation of avalanche occurrence with REM, N1 and N2, and a positive correlation ($\rho_{av,N3} = 0.38$) between avalanches and N3 (as we expect looking at density behavior in Fig. 5A).

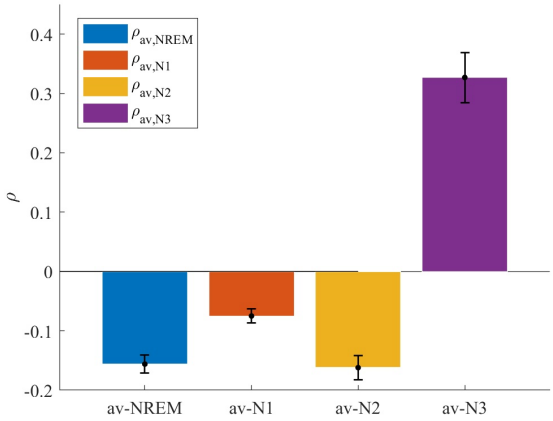

Fig. 6 The mean Pearson correlation coefficients $\rho_{x,y}$, see eq. (2), averaged over all the subjects, between avalanches occurrence and macrostructure sleep stages (namely REM,N1,N2,N3). The bar is the standard error of the mean correlation coefficient over subjects. P-value < 2.23e-308 for all considered correlations for all 10 subjects.

3.3 AVALANCHES DISTRIBUTION AND SLEEP MICROSTRUCTURE

Even though critical avalanche dynamics has a spatio-temporal structure that is scale-free from few milliseconds up to few seconds (see **Figs. 2, 3, 4**), we found correlations between the avalanches' occurrence and the sleep microstructural architecture dictated by the CAP dynamics, that have a characteristic time scale from few seconds to minutes. We measure the Pearson correlation coefficients between avalanches occurrence and sleep CAP microstates (see eq. (2)), and, in addition

, we qualitatively look at the time course of the density of phase A (and subtype A1) together with density of avalanches.

Fig. 7 shows the *Pearson correlations* of avalanches' occurrence with all the CAP A phases, the CAP A subtypes A1, A2, A3, CAP B phases and NCAP periods, as defined by eq.(2), averaged over all the subjects. These analyses show that the occurrence of avalanches during sleep is not casual but it is strictly related to the phases A of CAP and in particular A1. By counterpart we observed a negative or almost null correlation with NCAP periods and phases B across all subjects.

As shown in the **Fig. 8** for a representative subject (#1), there is a good time correspondence between the time course of the density of avalanches $F_{av}(t)$ as defined in (1) and the CAP phase A distribution over night, i.e. $F_A(t) = \frac{u_A(t)}{u_0}$ measured as the fraction of time occupied by phase A in each time bin of T=10 sec (and also density of subtype CAP-A1 is $F_{A1}(t)$).

We noticed that, with sleep deepening, the progressive increase of CAP density accompanied the gradual increase of avalanches' density. CAP cycles physiological increase during stages N2 and N3, indirectly leads to a reduction of time occupied by NCAP sleep. Furthermore, during the deepest stages of NREM sleep, CAP cycles typically present shorter phases B. These changes in the sleeping brain dynamics lastly sustain the observed increase of avalanches' density.

For all the subjects, we pooled the percentage of CAP A-phases and subtypes (A1, A2 and A3) over the TST and the percentage of phase A (or subtypes) occupied by avalanches

$$\langle F_{av} \rangle A = \frac{Time\ (A,av)}{Time\ (A)} \quad (7)$$

While the percentage of phase A occupied by avalanches is about 42.16%, the percentage of sleep time occupied by avalanches is 19,21%. Interestingly, CAP phase A1 are even more rich in avalanches compared to CAP A phases A2 and A3 (53,32% versus 43,84% and 27,72% respectively).

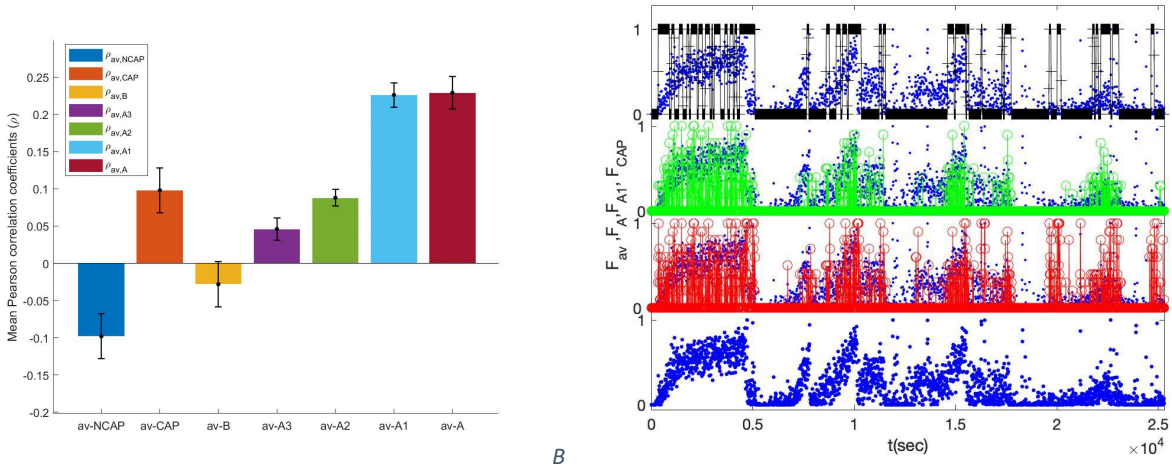

Fig. 7 A) The mean Pearson correlation coefficients $\rho_{x,y}$, see eq. (2), averaged over all the subjects, between avalanches occurrence and microstructure features (namely NCAP, CAP, B, A3,A2,A1, and all A phases). The bar is the standard error of the mean correlation coefficient over subjects. P-value < 2.23e-308 for all considered correlations, for all 10 subjects. B) Density of avalanches vrs. density of CAP phases as function of time in subject #1: density of avalanches in blue, density of phase A in red, density of phase A1 in green , density of CAP in black.

DISCUSSION

To the best of our knowledge, this is the first study exploring the scaling relation among critical exponents of neural avalanches during sleep. The exponent of average size as a function of duration has been studied in many in-vitro and animal awake preparations, but this is the first time it has been measured in human sleep. It's notable that the value of this exponent during sleep is in agreement with the Branching Process prediction k=2 (i.e the MF-DP universality class), since there is a large debate on the value of this exponent [Carvalho 2021].

Moreover, to the best of our knowledge, this is the first study exploring the correlation between sleep dynamics at both macro and microstructure level and avalanches. We introduced a novel measure, the density of avalanches as a function of time, representative of the amount of avalanches per time unit, and we explored the relationships between this parameter and the sleep hypnogram architecture and sleep stages. In addition, on a more microscopic scale, we study the Pearson correlation coefficient between the avalanche occurrence and the microstructure (CAP) features of sleep. The strongest positive correlation arose between avalanches and N3 sleep stage. In parallel, a milder

positive correlation coefficient was revealed between avalanche and CAP phases A, specifically with CAP subtypes A1, whilst, conversely, a negative correlation was observed between avalanche and NCAP sleep and an almost null relationship with phases B. Besides, our results highlighted a fascinating behavior of avalanches across night: their density gradually increases with sleep deepening, while it rapidly wanes when sleep-promoting forces decrease. In this framework we can hypothesize that avalanches in the sleeping brain actively contribute to sleep development.

Overall, our findings, while confirming previous assumptions on critical dynamics beyond sleep stages transitions, expand the current knowledge as they provide the evidence of a link between the avalanches occurrence, slow-wave sleep dynamics, sleep transitions and phase A occurrence, during NREM sleep. This is not trivial, as CAP is considered one of the major guardians of NREM sleep, allowing the brain to react dynamically to any external perturbation and contributing to the cognitive consolidation processes occurring in sleep.

Criticality and the sleeping brain dynamics

There is evidence that the human brain operates close to a critical regime both in resting wakefulness and during sleep [Priesmann et al 2013, Bocaccio et al. 2019, Allegrini et al.2013, Allegrini et al. 2015], and that sleep exerts a crucial role to re-tune brain dynamics towards criticality [Meisel et al. 2013, Meisel et al 2017]. Presently, we explore neural avalanches, and the scaling relation among critical exponents, in overnight polysomnographic recordings in human healthy subjects. Notably, the distributions of the avalanches' size and duration are well described by a power law, followed by a cut-off, both at single subject and group level analyses. The estimated critical exponents are $\tau = 1.42$, $\beta = 1.83$, almost close to the branching process prediction $\tau = 3/2$, $\beta = 2$. Another important exponent is the slope k of average size as a function of duration, in (5), related to τ, β by the scaling relation (6). It's a debated issue [Miller et al 2019, Fontenele 2019, Carvalho 2021, Fosque 2021] if the exponent k measured experimentally, from (5) and from scaling relationship (6), is a value compatible with the prediction $k = 2$ of the branching process, ie. the MF-DP universality

class, which has been the canonical model employed to understand brain criticality. Some experimental measurement of k not compatible with the value of MF-DP raised the question that a different model, with a different phase transition, might be required to explain the critical brain data [Fontenele 2019, Carvalho 2021, Fosque 2021]. Notably herein, we found that the value k predicted from the scaling relation (6) is close to k=2, and moreover, for each subject and for the group, the average size $\langle S \rangle$ as a function of duration in (5) has a slope k close to 2 (before the cut-off regime). Here we found that slope $k \simeq 1.3$ (different from MF-DP, and close to the value of some experimental animal measurements in [Fontanele 2019]) only holds in the region where P(S) and P(T) has the cut-off , therefore might be related to an effect of finite-size, i.e. a limited number of electrodes or limited statistics. Our findings are in line with Miller et al. (2019), who by measuring the avalanches in the ongoing local field potential of awake monkey, concluded that the slope relationship for avalanche size and duration identifies a scaling exponent k close to 2, in agreement with branching process, in the region when P(S) and P(T) support power law regimes (while $k \simeq 1 - 1.5$ in the cut-off regime and at temporal resolution that do not support power law regimes). Overall, our results support the idea that the branching process class may be a right framework for describing brain criticality. While the scaling relation (6) has already been verified in different brain criticality experiments [Fontanele 2019, Miller 2019, Fosque 2021], this is the first time that it has been explored during sleep.

Avalanches and sleep macrostructures

The relationship between neural avalanches and sleep stages has attracted much attention [Priesmann et al 2013, Allegrini et al 2013, Allegrini et al 2015, Bocaccio et al 2019]. Avalanches dynamics from human intracranial depth recordings [Priesmann et al 2013] indicated that size and duration avalanche's distribution approximated a similar power law behavior during the sleep-wake cycle, but with fewer large avalanches for REM sleep than for SWS (N2 and N3). Similarly, whole-brain fMRI data analyses confirmed a robust critical or near-critical behavior moving from wakefulness to deep sleep stages, with some small differences with respect to the exponent of power law distribution of

avalanches' size (in particular between wakefulness and stage N2) [Boccaccio et al., 2019]. However, as [Allegrini et al 2015] notes, although some significance in the small deviations among avalanches' distribution can be found in different sleep stages, the distributions are visually remarkably similar. Moreover, in some cases the differences seem to correlate with a numerosity difference (the time spent in N2 is much larger than the time spent in REM sleep) (Allegrini et al., 2015).

Here, to study changes in the avalanches dynamics across sleep stages we moved beyond the shape of the avalanches distribution and we introduced a novel quantity, the ***avalanches' density*** defined as the fraction of time occupied by avalanches, whose evolution in time has never been explored so far. We found that avalanche density markedly and progressively increases with NREM sleep stages N2 and N3 and, specifically, during periods of sleep deepening (descending slope of sleep cycles), in parallel with the increase of slow-waves. On the contrary, the abrupt decrease of avalanches' density during the ascending slope of sleep cycles suggests a negative influence from REM-on/wakefulness circuits with respect to their appearance. The different behavior of avalanche density during the descending and ascending slopes of the sleep cycles is an original finding, despite the crucial role of these dynamics in the sleep regulatory process. In terms of sleep physiology, the descending and ascending slopes of sleep cycles are markedly different: during the descending slope, sleep-promoting forces are stronger, the thalamo-cortical system works in the burst-firing mode and brainstem cholinergic pathways are tonically repressed. Conversely, during the ascending slope, the NREM driving forces become weaker, sleep is more vulnerable towards pro-arousal intrusions and REM-promoting outputs prevail (Halasz et al, 2004). With this in mind, our data suggest that the avalanche density is not casual across the sleep cycles but instead contributes to define and sustain the dynamical interplay between sleep-wake promoting networks.

Avalanches and sleep microstructure

Sleep architecture is composed of numerous oscillatory activities, including, above all, CAP, that, with a time scale of seconds or minutes, accompany stage shifts and contribute to the organization of

sleep cycles. Our results demonstrated a mild positive correlation between CAP and avalanche occurrence, while a negative relation was revealed between occurrence of avalanches and NCAP sleep. CAP is a periodic EEG activity that translates a state of brain instability, which is characterized by the alternation of phases of higher amplitude (CAP phases A, 'activation phases') separated by periods of lower amplitude EEG (CAP phases B, 'de-activation phases'). Conversely, NCAP is defined as a period of sustained physiologic stability. Technically, the absence of CAP cycles for more than 60 seconds is scored as NCAP, while CAP cycles separated by intervals from 2 to 60 seconds compose a CAP sequence and build the 'CAP sleep' (Terzano et al, Atlas CAP scoring, 2001). CAP phases A can be further subdivided into three subtypes: A1, A2 and A3. Isolated A1 phases, not followed by a subsequent phase A within 60 seconds, are scored as NCAP, confirming that the dynamic interplay between phases of activation/baseline is key characteristic of the CAP framework. Of note, the avalanches are related to the critical edge of a synchronization phase transition [Di Santo et al. 2018, Scarpetta et al. 2014], and, therefore, critical alternation of periods of collective synchronization (up state composted of avalanches) and desynchronization is among their rational organization. Although the definition of avalanches (related with large non-gaussian fluctuations of normalized sum of signals) is, in principle, not related with definition of CAP phase A, and their time scale is drastically different, our results show that neural avalanches are correlated with the occurrence of CAP phase A. The strongest association emerged between avalanches and CAP A1 subtypes, with minor positive correlation with subtypes A2 and A3 (**Fig. 7**).

Interestingly, as shown in **Fig. 7**, the association between avalanches and CAP phases A is even more significant than the one with CAP itself. We speculated that this could be due to the opposite significance of CAP phase B with respect to sleep dynamic. Phases B are parts of CAP cycles and electrophysiologically are characterized by the rebound of background EEG activity after the strong 'activation' driven by phases A. Compare to phases A, phases B could be described as 'lower arousal reactions' or vehicles of deactivation (Parrino et al., 2012 *Sleep Med Rev.*). Phases B are automatically included in the evaluation of CAP but their evaluation is excluded in the counts of

phases A. Interestingly, no significant correlation was observed between avalanches and phases B, further confirming our assumption about the relationship between phases A and avalanches.

CAP subtypes A1 physiologically prevail in the first half of the night and, during the descending slope of each sleep cycle, boosting or maintaining SWS. Similarly, avalanche density decreases moving from firsts to lasts sleep cycles and it also presents a very different behavior in the ascending versus descending slope of sleep cycles. Hence, both CAP phase A and avalanches follow a physiological homeostatic decay throughout the night and, apparently, they both contribute to the build-up of the deepest stages of NREM sleep.

Avalanches, CAP and learning mechanisms: an intriguing hypothesis It has been suggested that CAP subtypes A1 might play a role in the sleep-dependent learning processes (Ferri et al, 2008) and it is well-known that sleep is crucial to renormalize synaptic weight and to preserve cognition (Cirelli and Tononi, 2021). During sleep, the excess of novel synaptic connections, acquired during the day, would risk saturating brain reserves and thus a sleep-dependent renormalization took place (synaptic down-selection), to restore balance. Brain is an example of self-organized critical system, meaning that it continuously adjusts its critical level to the optimal one for its correct functioning. According to our results and in line with previous observations, given the large amount of avalanches during the night, we hypothesize that sleep exerts a pivotal role in modulating the brain critical restoration. On parallel, the positive association between stage N3, CAP subtypes A1 and avalanches, might indicate that both CAP-A1 and SWS actively contribute to the brain critical process and its modulation. Taken together, these observations might suggest that sleep supports at multiple levels (macro- and microstructure), the self-organization of brain near criticality, lastly favoring sleep-dependent learning mechanisms. This idea is in line with previous hypothesis (Scarpetta et al, 2014, Scarpetta 2019) that, during the up/down alternation, the periods of high activity (up states), which, at a finer temporal scale, are made of a sequence of scale-free avalanches, correspond to an intermittent reactivation of the stored spatiotemporal patterns (useful for memory consolidation). Scale free

avalanches in this scenario are the signature of a system at the critical edge between quiescence and sustained replay of spatio-temporal attractors previously learned.

Study limitations

Our study presents some limitations. The sample size is limited to ten healthy sleepers and wider samples are advisable to validate our exploratory results. However, methodology was meticulous and sleep scoring was manually performed by certified somnologists with strong expertise in the field. Our scientific conclusions are limited by the fact that avalanches and sleep oscillations were recorded by scalp EEG. Nevertheless, this was inevitable as we enrolled healthy volunteers, and more invasive techniques (e.g. icEEG) were not allowed.

SUPPLEMENTARY MATERIAL:

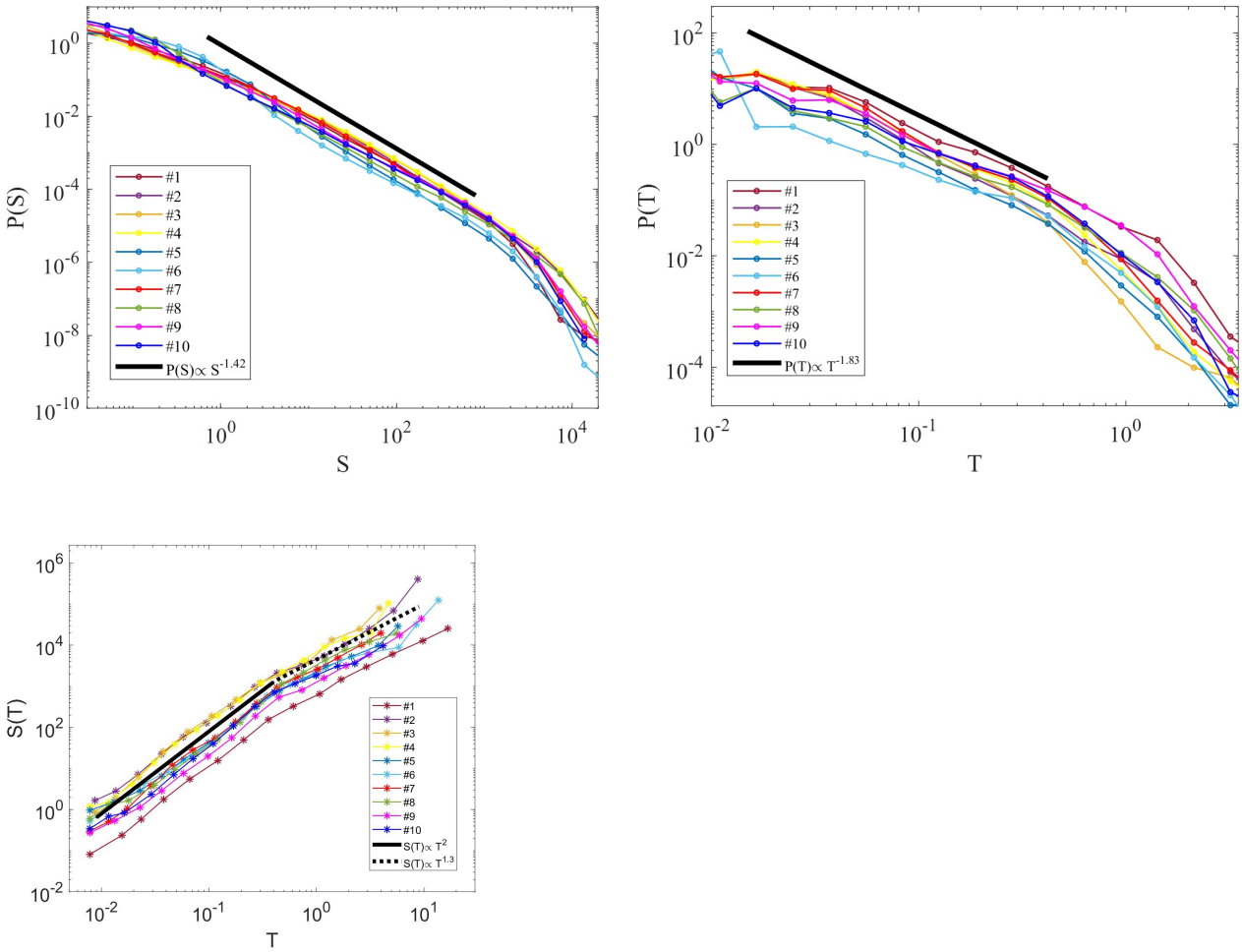

Supplementary **Fig. S1**

Avalanche's size and duration distribution for all the 10 subjects. The average size as a function of duration is well described by $\langle S \rangle(T) \propto T^k$ with $k = 2$ (black continuous line) for all single subjects up to a T^* where $P(T)$ has the cut-off regime. A slope $k = 1.3$ (black dotted line) is shown as a guide for eye at $T > T^*$.

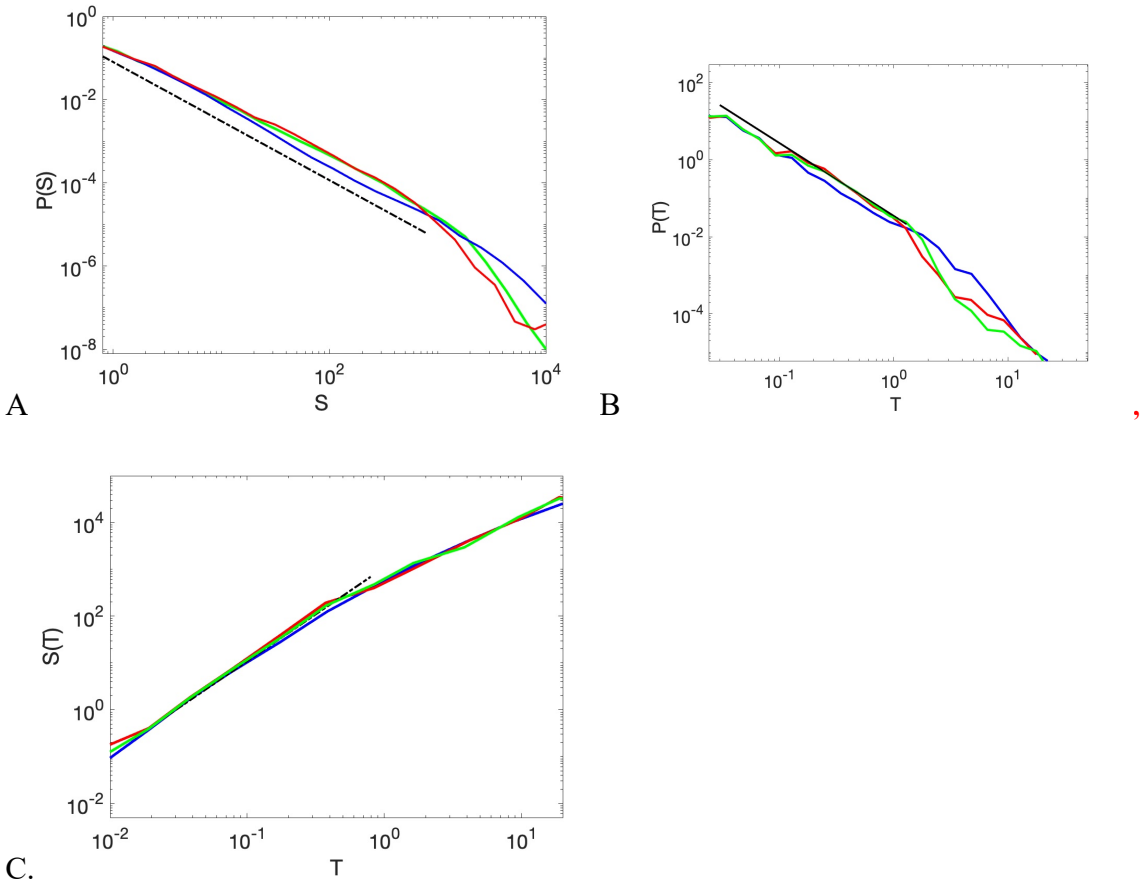

FIG. S2 Avalanche's size (**A**) and duration distribution (**B**) for subject #1, for different values of threshold in avalanche definition ($\vartheta = \pm 1$ SD blue, $\vartheta = \pm 2$ SD green, and $\vartheta = \pm 3$ SD red). The dotted black line is a guide for eyes, with the same slope used in Fig.2. The average size as a function of duration (**panel C**) is well described by $\langle S \rangle(T) \propto T^k$ with $k = 2$ (black continuous line) for all three thresholds ($\vartheta = \pm 1$ SD blue, $\vartheta = \pm 2$ SD green, and $\vartheta = \pm 3$ SD red) up to a T^* where $P(T)$ has the cut-off regime.

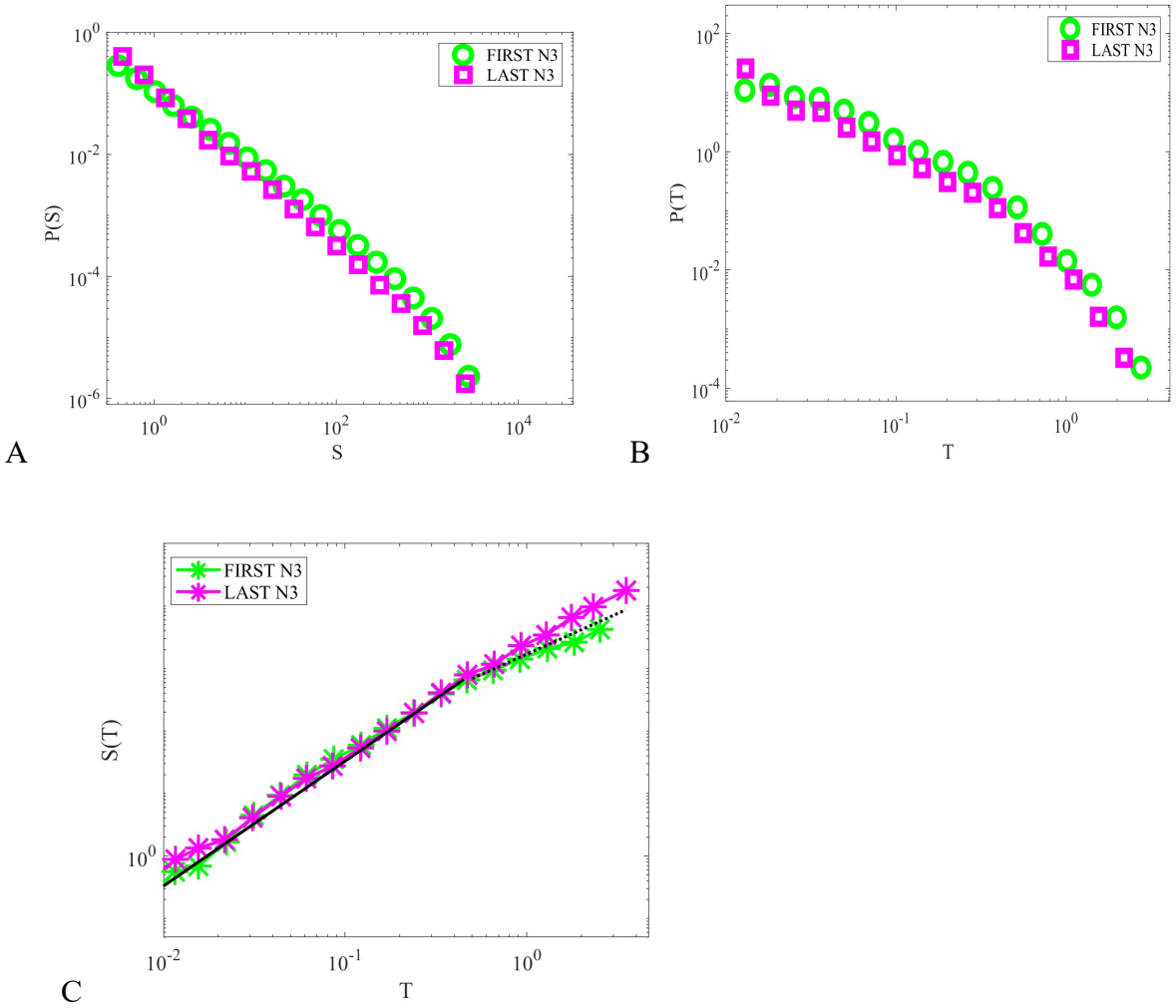

Fig. S3 (A,B) Distribution of size and duration for avalanches in the FIRST N3 (green) and the LAST N3(magenta). (C,D) Mean size as a function of duration for avalanches of all subjects in the FIRST N3 (C) and t LAST N3 stage (D). The avalanche statistics follows (5) with $k = 2$, up to the cutoff regime, in both cases. The slope $k = 2$ (black continuos line) is shown as a guide for eye at $T < T^*$, and a slope 1.3 (dotted line) in the cut-off regime for comparison.

Bibliography:

1. Berry R. B. *et al. The AASM Manual for the Scoring of Sleep and Associated Events*. *American Academy of Sleep Medicine* **53,** (2013).

2. Schulz H. Rethinking sleep analysis. *Journal of Clinical Sleep Medicine* **4,** 99–103 (2008).

3. Iber C., Ancoli-Israel S., Chesson A. & Quan S. *The AASM Manual for the Scoring of Sleep and Associated Events: Rules, Terminology and Technical Specifications*. (American Academy of Sleep Medicine, 2007).

4. L. Parrino, A. Smerieri, M. Rossi, M.G. Terzano, Relationship of slow and rapid EEG components of CAP to ASDA arousals in normal sleep, Sleep 24 (2001) 881–885.

5. Farina B. *et al.* Microstructure of sleep in depressed patients according to the cyclic alternating pattern. *J. Affect. Disord.* **77,** 227–235 (2003).

6. Terzano M.G. *et al.* Erratum: 'Atlas, rules, and recording techniques for the scoring of cyclic alternating pattern (CAP) in human sleep' (Sleep Medicine (2001) vol. 2 (6) (537-553)). *Sleep Med.* **3,** 185 (2002).

7. Parrino L., Ferri R., Bruni O. & Terzano M. G. Cyclic alternating pattern (CAP): The marker of sleep instability. *Sleep Med. Rev.* **16,** 27–45 (2012).

8. Meisel, C., Olbrich, E., Shriki, O., & Achermann, P. (2013). Fading signatures of critical brain dynamics during sustained wakefulness in humans. *Journal of Neuroscience*, *33*(44), 17363-17372.

9. Fagerholm, E. D., Lorenz, R., Scott, G., Dinov, M., Hellyer, P. J., Mirzaei, N., ... & Leech, R. (2015). Cascades and cognitive state: focused attention incurs subcritical dynamics. *Journal of Neuroscience*, *35*(11), 4626-4634.

10. Shriki, O., Alstott, J., Carver, F., Holroyd, T., Henson, R. N., Smith, M. L., ... & Plenz, D. (2013). Neuronal avalanches in the resting MEG of the human brain. *Journal of Neuroscience*, *33*(16), 7079-7090.

11. S.H. Gautam, T.T. Hoang, K. Mc Clanahan, S.K. Grady, and W.L. Shew, "Maximizing sensory dynamic range by tuning the cortical state to criticality," PLoS Comp. Bio. 11, e1004576 (2015)

12. Beggs, Plenz *Neuronal avalanches in neocortical circuits* J Neurosci. 2003 Dec 3;23(35):11167-77.

13. Petermann, T., Thiagarajan, T. C., Lebedev, M. A., Nicolelis, M. A., Chialvo, D. R., & Plenz, D. (2009). Spontaneous cortical activity in awake monkeys composed of neuronal avalanches. *Proceedings of the National Academy of Sciences*, *106*(37), 15921-15926.

14. Terzano, M. G., Parrino, L., Boselli, M., Smerieri, A., & Spaggiari, M. C. (2000). CAP components and EEG synchronization in the first 3 sleep cycles. *Clinical neurophysiology*, *111*(2), 283-290.

15. Shew, W. L., Clawson, W. P., Pobst, J., Karimipanah, Y., Wright, N. C., & Wessel, R. (2015). Adaptation to sensory input tunes visual cortex to criticality. *Nature Physics*, *11*(8), 659-663.

16. Ma, Z., Turrigiano, G. G., Wessel, R., & Hengen, K. B. (2019). Cortical circuit dynamics are homeostatically tuned to criticality in vivo. *Neuron*, *104*(4), 655-664.

17. Chialvo, D. R. (2010). Emergent complex neural dynamics. *Nature physics*, *6*(10), 744-750.

Massobrio Paolo, de Arcangelis Lucilla, Pasquale Valentina, Jensen Henrik J., Plenz Dietmar (2015) Criticality as a signature of healthy neural systems, Front. Syst. Neurosci. 9.

18. Kinouchi, O., & Copelli, M. (2006). Optimal dynamical range of excitable networks at criticality. *Nature physics*, *2*(5), 348-351.

19. Hesse, J., & Gross, T. (2014). Self-organized criticality as a fundamental property of neural systems. *Frontiers in systems neuroscience*, *8*, 166.

20. Shew, W. L., & Plenz, D. (2013). The functional benefits of criticality in the cortex. *The neuroscientist*, *19*(1), 88-100.

21. Touboul, J., & Destexhe, A. (2017). Power-law statistics and universal scaling in the absence of criticality. *Physical Review E*, *95*(1), 012413.

22. Serena di Santo, Pablo Villegas, Raffaella Burioni, and Miguel A. Muñoz; Landau–Ginzburg theory of cortex dynamics: Scale-free avalanches emerge at the edge of synchronization; PNAS February 13, 2018 115 (7) E1356-E1365

23. Ferri et al. 2008 Ferri R, Huber R, Aricò D, et al. The slow-wave components of the cyclic alternating pattern (CAP) have a role in sleep-related learning processes. *Neurosci Lett*. 2008;432(3):228-231. doi:10.1016/j.neulet.2007.12.025

24. L. Fosque et al. (2021) Evidence for Quasicritical Brain Dynamics, Physica Review E

25. Jeldtoft Jensen, H. (1998). Self-Organized Criticality. *Self-Organized Criticality*, 167.

26. Parrino, L., & Vaudano, A. E. (2018). The resilient brain and the guardians of sleep: new perspectives on old assumptions. *Sleep medicine reviews*, *39*, 98-107.

27. Scarpetta, S., & de Candia, A. (2013). Neural avalanches at the critical point between replay and non-replay of spatiotemporal patterns. *PLoS One*, *8*(6), e64162.

28. Scarpetta S. de Candia A (2014) Alternation of up and down states at a dynamical phase-transition of a neural network with spatiotemporal attractors. Front. Syst. Neurosci., 19 May 2014 | https://doi.org/10.3389/fnsys.2014.00088

29. Scarpetta, S. (2019). Critical Behavior and Memory Function in a Model of Spiking Neurons with a Reservoir of Spatio-Temporal Patterns. In: Tomen, N., Herrmann, J., Ernst, U. (eds) The Functional Role of Critical Dynamics in Neural Systems . *Springer Series on Bio- and Neurosystems, vol 11.* Springer, Cham. https://doi.org/10.1007/978-3-030-20965-0_10

30. Munoz, M. A. (2018). Colloquium: Criticality and dynamical scaling in living systems. *Reviews of Modern Physics*, *90*(3), 031001.

31. Yaghoubi, M., de Graaf, T., Orlandi, J. G., Girotto, F., Colicos, M. A., & Davidsen, J. (2018). Neuronal avalanche dynamics indicates different universality classes in neuronal cultures. *Scientific reports*, *8*(1), 1-11.

32. Meisel, C., Bailey, K., Achermann, P., & Plenz, D. (2017). Decline of long-range temporal correlations in the human brain during sustained wakefulness. *Scientific reports*, *7*(1), 1-11.

33. Allegrini P. et al PHYSICAL REVIEW E 92, 032808 (2015).

34. Allegrini P. et al. Chaos, Solitons Fractals 55, 32 (2013).

35. Wang, J. W., Lombardi, F., Zhang, X., Anaclet, C., & Ivanov, P. C. (2019). Non-equilibrium critical dynamics of bursts in θ and δ rhythms as fundamental characteristic of sleep and wake micro-architecture. *PLoS computational biology*, *15*(11), e1007268.

36. Lombardi, F., Wang, J. W., Zhang, X., & Ivanov, P. C. (2020). Power-law correlations and coupling of active and quiet states underlie a class of complex systems with self-organization at criticality. In *EPJ web of conferences* (Vol. 230, p. 00005). EPJ Web of Conferences.

37. J. Alstott, E. Bullmore, and D. Plenz, A Python package for analysis of heavy-tailed distributions, Plos One 9, e95816 (2014)

38. J. P. Sethna, K. A. Dahmen, and C. R. Myers, Crackling noise, Nature (London) 410, 242 (2001)

39. Scarpetta, S., Apicella, I., Minati, L., & de Candia, A. (2018). Hysteresis, neural avalanches, and critical behavior near a first-order transition of a spiking neural network. *Physical Review E*, *97*(6), 062305.

40. Friedman, N., Ito, S., Brinkman, B. A., Shimono, M., DeVille, R. L., Dahmen, K. A., ... & Butler, T. C. (2012). Universal critical dynamics in high resolution neuronal avalanche data. *Physical review letters*, *108*(20), 208102.

41. Mariani, B., Nicoletti, G., Bisio, M., Maschietto, M., Oboe, R., Leparulo, A., Suweis, S., & Vassanelli, S. (2021). Neuronal Avalanches Across the Rat Somatosensory Barrel Cortex and the Effect of Single Whisker Stimulation. *Frontiers in systems neuroscience*, *15*, 709677. https://doi.org/10.3389/fnsys.2021.709677

42.

43. Fontenele, A. J., de Vasconcelos, N. A., Feliciano, T., Aguiar, L. A., Soares-Cunha, C., Coimbra, B., ... & Copelli, M. (2019). Criticality between cortical states. *Physical review letters*, *122*(20), 208101.

44. Miller SR, Yu S, Plenz D. The scale-invariant, temporal profile of neuronal avalanches in relation to cortical γ-oscillations. Sci Rep. 2019 Nov 11;9(1):16403. doi: 10.1038/s41598-019-52326-y. PMID: 31712632; PMCID: PMC6848117.

45. Carvalho TTA, Fontenele AJ, Girardi-Schappo M, Feliciano T, Aguiar LAA, Silva TPL, de Vasconcelos NAP, Carelli PV and Copelli M (2021) Subsampled Directed-Percolation Models Explain Scaling Relations Experimentally Observed in the Brain. Front. Neural Circuits 14:576727. doi: 10.3389/fncir.2020.576727

46. Shew, W. L., Clawson, W. P., Pobst, J., Karimipanah, Y., Wright, N. C., & Wessel, R. (2015). Adaptation to sensory input tunes visual cortex to criticality. *Nature Physics*, *11*(8), 659-663.

47. Massobrio, P., de Arcangelis, L., Pasquale, V., Jensen, H. J., & Plenz, D. (2015). Criticality as a signature of healthy neural systems. *Frontiers in systems neuroscience*, *9*, 22.

48. Cocchi, L., Gollo, L. L., Zalesky, A., & Breakspear, M. (2017). Criticality in the brain: A synthesis of neurobiology, models and cognition. *Progress in neurobiology*, *158*, 132-152.

49. Fraiman, D., & Chialvo, D. R. (2012). What kind of noise is brain noise: anomalous scaling behavior of the resting brain activity fluctuations. *Frontiers in physiology*, *3*, 307.

50. Tagliazucchi, E., Balenzuela, P., Fraiman, D., & Chialvo, D. R. (2012). Criticality in large-scale brain fMRI dynamics unveiled by a novel point process analysis. *Frontiers in physiology*, *3*, 15.

51. Haimovici, A., Tagliazucchi, E., Balenzuela, P., & Chialvo, D. R. (2013). Brain organization into resting state networks emerges at criticality on a model of the human connectome. *Physical review letters*, *110*(17), 178101.

52. Bocaccio, H., Pallavicini, C., Castro, M. N., Sánchez, S. M., De Pino, G., Laufs, H., ... & Tagliazucchi, E. (2019). The avalanche-like behaviour of large-scale haemodynamic activity from wakefulness to deep sleep. *Journal of the Royal Society Interface*, *16*(158), 20190262.

53. Priesemann, V., Valderrama, M., Wibral, M., and Le Van Quyen, M. (2013). Neuronal avalanches differ from wakefulness to deep sleep–evidence from intracranial depth recordings in humans. *PLoS Comput. Biol.* 9:e1002985. doi: 10.1371/journal.pcbi.1002985

54. Solovey, G., Miller, K. J., Ojemann, J. G., Magnasco, M. O., and Cecchi, G. A. (2012). Self-regulated dynamical criticality in human ECoG. *Front. Integr. Neurosci.* 6:44. doi: 10.3389/fnint.2012.00044

55. Palva, J. M., Zhigalov, A., Hirvonen, J., Korhonen, O., Linkenkaer-Hansen, K., and Palva, S. (2013). Neuronal long-range temporal correlations and avalanche dynamics are correlated with behavioral scaling laws. *Proc. Natl. Acad. Sci. U S A* 110, 3585–3590. doi: 10.1073/pnas.1216855110

56. Thiagarajan, T. C., Lebedev, M. A., Nicolelis, M. A., & Plenz, D. (2010). Coherence potentials: loss-less, all-or-none network events in the cortex. *PLoS biology*, *8*(1), e1000278.

57. Lo, C. C., Chou, T., Penzel, T., Scammell, T. E., Strecker, R. E., Stanley, H. E., & Ivanov, P. C. (2004). Common scale-invariant patterns of sleep–wake transitions across mammalian species. *Proceedings of the National Academy of Sciences*, *101*(50), 17545-17548.

58. Cirelli C, Tononi G. The why and how of sleep-dependent synaptic down-selection [published online ahead of print, 2021 Mar 9]. *Semin Cell Dev Biol*. 2021;S1084-9521(21)00031-8. doi:10.1016/j.semcdb.2021.02.007

59. Steriade, M., Timofeev, I., and Grenier, F. (2001). Natural waking and sleep states: a view from inside neocortical neurons. J. Neurophysiol. *85*, 1969–1985.

60. Terzano MG, Parrino L, Smerieri A, Chervin R, Chokroverty S, Guilleminault C, Hirshkowitz M, Mahowald M, Moldofsky H, Rosa A, Thomas R, Walters A. Atlas, rules, and recording techniques for the scoring of cyclic alternating pattern (CAP) in human sleep. Sleep Med. 2002 Mar;3(2):187-99. doi: 10.1016/s1389-9457(02)00003-5. PMID: 14592244.